JOURNAL OF MATERIALS SCIENCE 20 (1985) 636–642

Study of the deformation behaviour of homogeneous materials by impression tests

H. Y. YU
Chung Cheng Institute of Technology, Tao-Yuan, Taiwan, Republic of China
M. A. IMAM, B. B. RATH
Naval Research Laboratory, Washington, DC 20375, USA

An impression test method and analytical procedure have been used to generate the flow characteristics of aluminium, copper, nickel and mild steel. Unlike conventional tests, the flow curves of these materials can be obtained by precise measurements of the displacement of a flat-ended circular cylinder into a specimen at predetermined speeds, during which the indenter makes an impression on the surface of the specimen as a function of the applied load. The depth of penetration at an equivalent stress, speed being constant, is found to be linearly dependent on the diameter of the indenter, varying over a range up to 2 mm in a typical metallographic sample. Thus a simple normalization of displacement with diameter makes the stress–penetration relation independent of indenter size. These results are compared with those obtained from conventional tests and the merits of evaluating parameters by impression tests are discussed.

1. Introduction

The use of a flat-ended circular cylinder punch to study the mechanical behaviour of materials was first proposed by Kirsch in 1891 [1]. He evaluated the hardness by the load required to force a 5 mm diameter hard steel punch into a specimen to a depth of 0.1 mm. Recently Chu and Li [2] used an impression test method for a localized stress relaxation. In this test, a small flat-ended cylindrical punch was impressed onto the surface of the LiF single crystal using an Instron machine with constant cross-head speed. At a predetermined depth of the impression the cross-head was stopped and the load relaxation with time was recorded. It was found that the velocity–stress exponent for the dislocation motion obtained in this way was identical to that obtained by conventional methods of stress relaxation measurements [3]. It appears that upon a very large (semi-infinite) specimen the punch exerts a tension and elongation along the top surface by pushing the material down. At first, there is an elastic deformation front which moves below the indenter and is followed by a curved zone of plastic deformation as the pressure increases. Exploration of an axial section by O'Neill and Greenwood [4] using the 120° diamond cone test revealed local hardening gradients forming a "zone of influence" round the indentation with dimensions compatible with the size of the punch. Furthermore, using an etch-pit technique to reveal the plastic zone under the circular punch impression of the LiF single crystal, Yu and Li [5] showed that the size of the plastic zone is about the same as the indenter diameter.

The material under a loaded indenter is subject to combined stress and it is known that hydrostatic pressure will not, by itself, produce plastic deformation. Various stress criteria for the onset of plastic flow have been derived (Tresca–Mohr, Haber–Mises, Haar–Harman) and their application to indentation by a flat-ended cylindrical punch has been made by several investigators [6–10]. When a flat-ended cylindrical punch is applied to an ideally plastic metal, the shear stresses at its sharp edges

0022–2461/85 $03.00 + .12

become very high and plastic flow commences at about 1.1 σ_y (σ_y being the yield stress), although the rest of the material only yielded elastically. As the load increases plastic flow spreads and a general permanent indentation occurs.

Using a spherical indenter for the hardness test on annealed copper and mild steel, Tabor [11, 12] demonstrated that there is close agreement between the stress–strain curves and the hardness results. In order to obtain the stress–strain relation through the hardness measurements the processes involved are: (1) measure the Vickers hardness of a metal that has been deformed by various amounts in order to obtain the relationship between the hardness number, the amount of deformation or strain, ϵ, and the elastic limit, σ_e, at any stage, (2) Brinell impressions of various sizes are then made on the surface of the specimen, followed by Vickers hardness measurements made with a small load very near the edge of the Brinell indentation, (3) correlate the size of the impression, d/D, (where d is the indentation chordal diameter and D is the diameter of the ball), the mean stress, P_m, of the impression, the elastic limit, σ_e, and strain, ϵ. For mild steels and annealed copper, they found a relationship described as:

$$\sigma_e = P_m/2.8 \quad (1)$$

$$\epsilon = 0.2\, d/D \quad (2)$$

From hardness measurements and using Equations 1 and 2, σ_e against ϵ was plotted and good agreement was found between this result and known compression stress–strain curve.

Besides the Brinell hardness test, Atkins and Tabor [12] also showed that the stress–strain behaviour can be evaluated from hardness measurements with a conical indenter. The procedures involved for this are: (1) compress several cylindrical specimens to different degrees of strain, (2) measure the hardness with different angles of diamond cone in a Vickers hardness instrument, (3) for each cone angle θ, a proportional constant, C_θ, which is a function of cone angle, is determined such that:

$$P_m = C_\theta \sigma_e \quad (3)$$

and (4) a representative strain, ϵ_θ, which is associated with each cone is determined by finding the the best fit to the known stress–strain curves of the material. This is done in one of two ways: (1) investigating the change of hardness and C_θ with cone angle for a given amount of work-hardening, and (2) investigating the change of hardness and C_θ with work-hardening for a given cone angle. By using the conversion data of C_θ and ϵ_θ, the stress–strain relationships of mild steels and copper were obtained which agreed, within 7%, with the available stress–strain data. Despite the lengthy process and the error introduced by elastic recovery [13] during hardness measurements, this procedure provided an alternative method to construct the stress–strain curve for the materials. The purpose of this investigation is to develop a simple method for evaluating flow characteristics of metals and alloys using impression tests and an appropriate analytical procedure. In addition to the simplicity and time effectiveness of this process, it is uniquely suited for determining deformation characteristics of weldments, materials with graded properties or for situations where material limitations prevent fabrication of larger samples for standard tensile tests.

2. Experimental procedure

The materials selected for the investigation were 1018 mild steel, commercially pure aluminium, nickel and copper. Starting materials were annealed to remove all residual stresses. The annealing conditions and grain sizes for these materials are listed in Table I.

The samples for compression tests were prepared according to ASTM-E9-77 specifications for testing of metallic materials at room temperature. The samples used in this investigation were in the form of a cylinder, 13 mm in diameter and 26 mm long. For impression tests, the sample dimension requirements were not stringent as long as the two flat ends were parallel, and the sample height large enough to contain the plastic zone well within the sample. In this investigation samples, 13 mm thick with diameters ranging from 13 mm to 25 mm were used.

The testing arrangement for impression tests is shown schematically in Fig. 1. The flat-ended

TABLE I

Material	Annealing		Average grain size (μm)
	temperature (°C)	time (h)	
1018 mild steel	900	1	50
Al	350	1	40
Ni	500	1	20
Cu	600	1	35

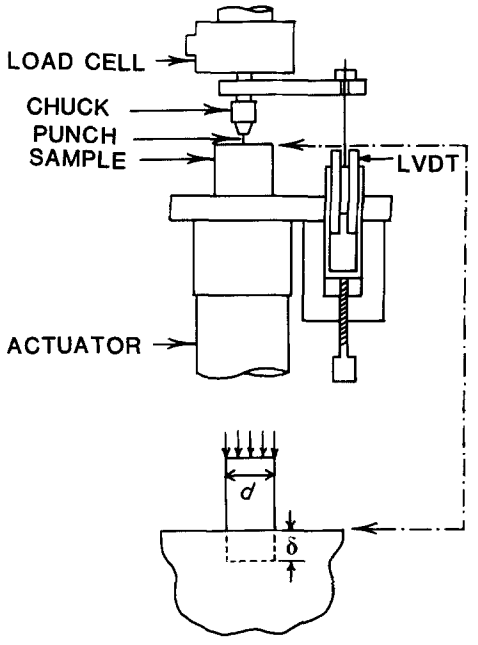

Figure 1 Schematic diagram of test arrangement for the impression test.

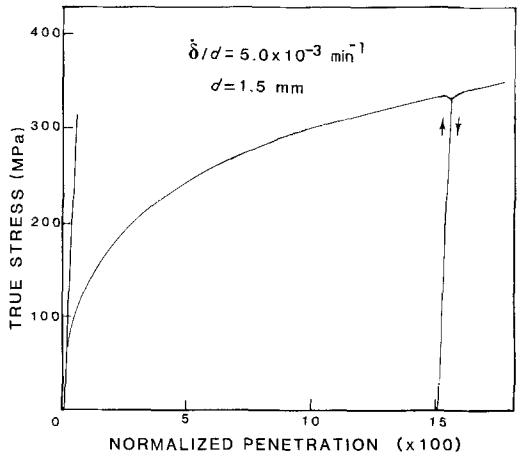

Figure 2 A typical true stress against normalized penetration curve of aluminum obtained by an impression test.

cylindrical punch was machined from Tungsten carbide rods. Three different puch diameters, 1 mm, 1.5 mm and 2 mm, were used for this study. The test was done at room temperature in a closed loop MTS hydraulic testing machine under stroke control conditions. The displacement of the punch or the penetration was recorded continuously from the output of an LVDT attached between the load cell and the sample.

For better accuracy strain gauges were used in the compression test to measure strains up to its limit of 2%. The strains up to 2% and beyond were also measured by the LVDT of the MTS machine. The samples, coated with both teflon and molybdenum disulphide to serve as lubricants, were placed on spherical-seated bearing blocks. The cross-head speed used in compression tests was 0.5 inch stroke movement for 6×10^3 sec which is equivalent to a strain rate of 5×10^{-3} min^{-1}.

For impression tests, the samples were placed on top of a compression platen attached to the actuator. The compression platen had a lubricated spherical seat and was held by a spring for self-alignment. The punch was forced into the specimens at a constant rate. The load signal from the MTS unit and the corresponding penetration signals from LVDT were recorded simultaneously during the test by an x–y recorder.

3. Results and discussion

A typical stress–penetration curve obtained for aluminium by an impression test is shown in Fig. 2. Similar to the true stress–true strain curves in the conventional compression test, Fig. 2 shows systematic work hardening in the plastic region. The unloading and reloading behaviour in the plastic region is very similar to those observed in conventional tests. The stress–penetration behaviour clearly suggests that an elastic deformation front initially forms ahead of the moving indenter, which at the elastic limit of the material gives way to a plastic zone which moves in a steady-state shape as the pressure continues to increase. It is suggested that a stagnant cap of increasingly strain-hardening material, having a curved or conical contour, eventually forms directly under the punch and produces a lower zone of radial compression [1]. The compressed materials follow the direction of least resistance and flow upwards towards the free surface resulting in the formation of a bulge at the free surface. The elastic–plastic boundary between the two zones can be determined by specialized metallographic etching techniques or recrystallization anneals on sectioned specimens [14].

The depth of penetration, δ, at an equivalent stress, speed being constant, is found to be linearly dependent on the diameter, D, of the indenter, varying over a range up to 2 mm in a typical metallographic sample. Thus, a simple normalization of displacement, δ, with diameter, D, makes the stress–penetration relation independent of indenter size. The results for 1018 mild steel and copper with 1 mm, 1.5 mm and 2 mm indenter diameters

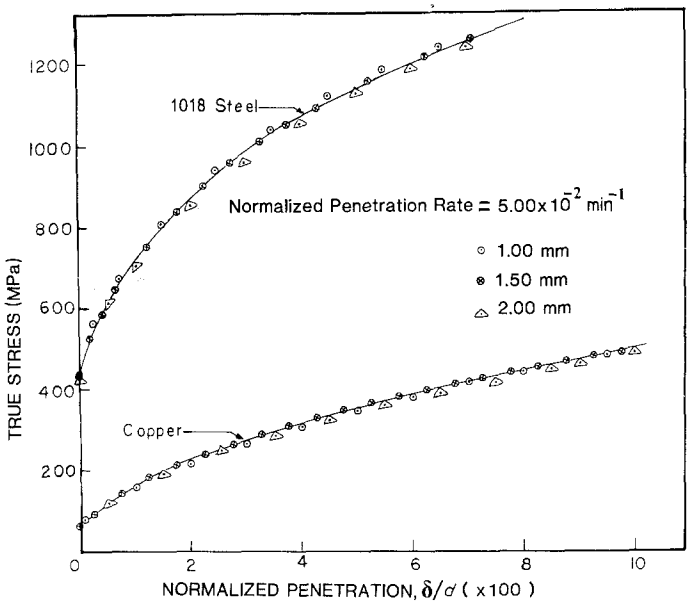

Figure 3 True stress against normalized penetration curve (strain-hardening region only) of 1018 mild steel and copper with indenter sizes of 1.00 mm, 1.50 mm, and 2.00 mm showing no effect on indenter size.

are shown in Fig. 3. The penetration speed for these tests was maintained at 5.08×10^{-3} min^{-1}. The results illustrate that, independent of material properties, a simple normalization of penetration depth by the indenter diameter consistently fall on the same curve. This observation is similar to the reported results on impression-creep tests [15, 16] which showed that the impression velocity, v, is linearly proportional to the indenter diameter.

In order to compare the results of impression and compression tests, the penetration speed for the 1.5 mm diameter indenter is choosen such that δ/D is nearly identical to the selected strain rate in compression tests. For this study the former was maintained at 5.08×10^{-3} min^{-1} while the latter at 5.0×10^{-3} min^{-1}. Based on the well-known experimental relationship between true stress and true strain, the uniform strain-hardening regions under both impression and compression tests are plotted on a log–log scale as shown in Figs. 4a and b. Results show that both tests confer to an identical strain exponent varying only by a different pre-exponential constant. This observation is consistent for four different materials examined in this

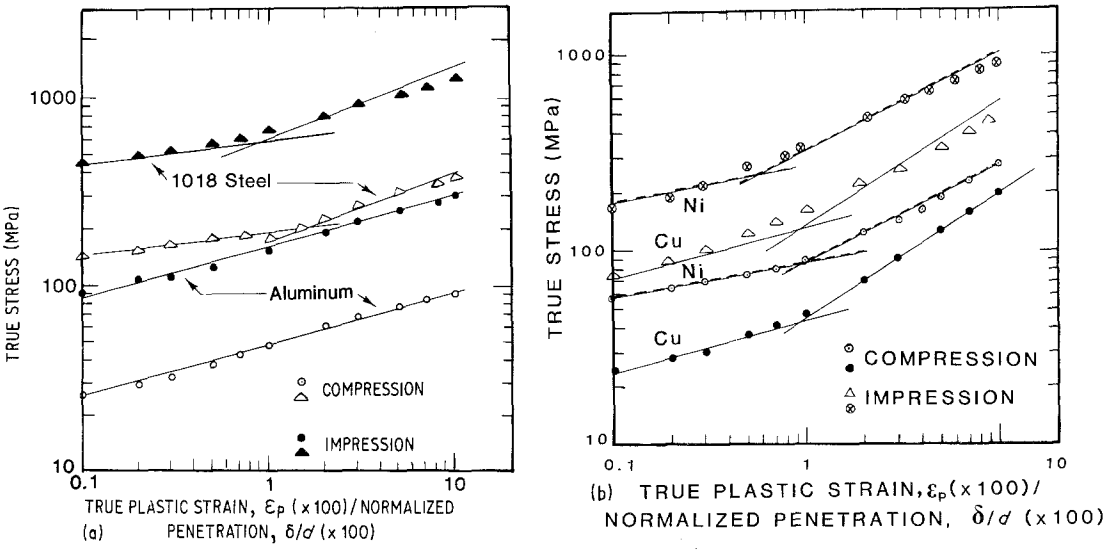

Figure 4 (a) Log–log plot of (strain-hardening region only) true stress against true strain/normalized penetration data for 1018 steel and aluminum. (b) Log–log plot of (strain-hardening region only) true stress against true strain/normalized penetration data for nickel and copper.

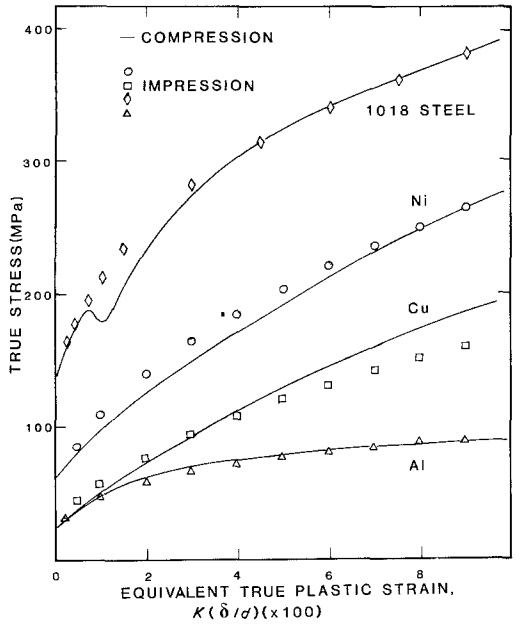

Figure 5 True stress against true strain/normalized penentration curves for 1018 steel, nickel, copper, and aluminium showing comparison between impression and compression tests.

investiagtion. It is interesting to note that the two strain exponent values seen for 1018 steel, nickel and copper, and the single value obtained for aluminium are constantly observed under both test conditions. Furthermore, the results of Fig. 4 suggest the following relationship between impression and compression tests which is similar to Equations 1 and 2:

$$P_m = c\sigma \tag{4}$$

$$\epsilon = k\frac{\delta}{D} \tag{5}$$

where P_m is impression stress, σ is compression stress, ϵ is true strain, δ/D is the normalized penetration depth, and c and k are constants. By linear square fit with one or two straight lines, one can find the constants c and k in Equations 4 and 5 respectively. Once c and k are found, the impression tests are performed again with penetration rate, $k(\dot{\delta}/D)$, equal to 5.08×10^{-3} min^{-1}. The results of these tests are plotted in Fig. 5. Fig. 5 shows the true stress–true strain (equivalent strain) plots for 1018 steel, aluminum, copper and nickel. When the impression curve is adjusted by dividing c to the stress P_m and the strain axis adjusted so that the $\epsilon = k(\delta/D)$, it is seen that there is close agreement between the stress–strain curves of compression tests and the impression results. The values c and k for mild steel, aluminum, copper and nickel are summarized in Table II. It is noted that c varies from 2.90 to 3.48 whereas k varies from 1.0 to 1.6. Thus the empirical Equations 4 and 5 should be calibrated if new material is tested.

TABLE II

Material	c	k
1018 steel	2.90	1.5
aluminum	3.48	1.0
copper	2.88	1.0
nickel	2.90	1.6

When the load increases plastic flow spreads and general permanent indentation occurs. According to Tabor [1] the mean pressure, P_m, across the face of the punch is given theoretically by $P_m \simeq 3\sigma_e$. This relationship assumes that the material has been strain hardened so that its yield point is no longer raised by straining. The ratio, c, between impression stress and compression stress found in this investigation is not widely different from the value 3. The ratio D/k is equivalent to the size of the plastic zone under the punch. Hence, with the value of k around 1, it means the plastic-zone size is about the same order as the indenter diameter, which is compatible with the experimental results for LiF [5] and copper [4].

The most common mathematical relationship used to express the true stress–true strain curve has the form

$$\sigma = \beta\epsilon^n \tag{6}$$

where c is the stress at $\epsilon = 1.0$ and n, the strain-hardening coefficient, is the slope of log–log plot of Equation 5. Substituting Equations 4 and 5 into Equation 6, gives

$$P_m = c\beta k^n\left(\frac{\delta}{D}\right)^n \tag{7}$$

Therefore, the strain-hardening coefficient, n, can be obtained from the slope of $\log P_m$ against $\log(\delta/d)$ plot regardless of the constants c and k.

It has been shown that the recovery of indentation during hardness test is elastic for both spherical [11] and conical indenters [13]. The elastic recovery can be readily seen in the present investigation as shown in Fig. 2, where the unload and reload curve follow the same slope. From the slope of the present test, an elastic modulus, E_{im}, for impression test has been obtained and reported

TABLE III

Material	Elastic modulus E in compression		Elastic modulus E_{im} in impression			
	(GPa)	(X 10^6psi)	(GPa)	(X 10^6psi)	$(E_{im}/E)_{exp}$	$(E_{im}/E)_{Th}$
1018 steel	195.1	(28.3)	326.8	(47.4)	1.67	1.43
AI	67.6	(9.8)	86.9	(12.6)	1.29	1.41
Cu	200.0	(29.0)	290.3	(42.1)	1.45	1.41
Ni	110.3	(16.0)	157.9	(22.9)	1.43	1.43

in Table III. The elastic stresses produced in a semi-infinite elastic solid by the indentation of a rigid, flat-ended circular cylinder punch of diameter, D, has been solved by Harding and Sneddon [10]. The relationship between the impression stress, P_m, on the pressed area to the depth, δ, below the free surface is given by

$$P_m = 4E/\pi(1-\nu^2)(\delta/D) \quad (8)$$

where E and ν are the modulus of elasticity and Poisson's ratio respectively. Using Equation 8, the elastic modulus for impression is given by

$$E_{im} = \frac{4}{\pi(1-\nu^2)} E \quad (9)$$

Taking Poisson's ratios for steel, aluminum, copper and nickel as 0.33, 0.31, 0.33 and 0.31 respectively, moduli were calculated and compared with the results of the present investigation as shown in Table III and plotted in Fig. 6. Results show that the ratio E_{im}/E for copper and nickel agrees very well with the theoretical value whereas for 1018 steel and aluminum the ratio is slightly off. The small difference involved in the ratio, E_{im}/E, for 1018 steel and aluminum may be attributed to the selection of the value of Poisson's ratio. Thus, this provides a simple method to evaluate the elastic modulus of a material.

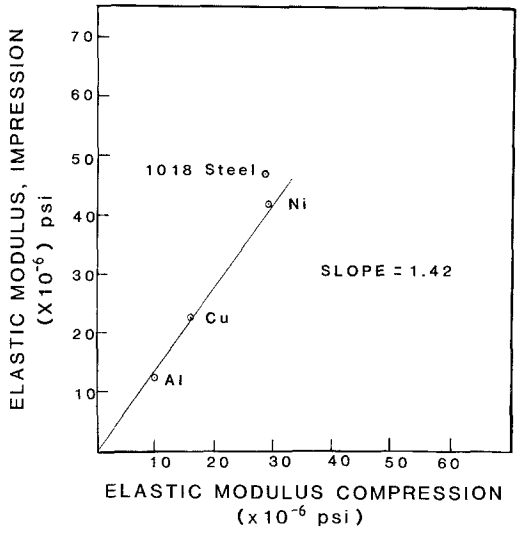

Figure 6 A plot of compression against impression tests moduli showing a linear relationship.

4. Summary

1. An impression test method and analytical procedure have been used to generate flow characteristics of a homogeneous material of annealed mild steel, aluminum, nickel and copper.

2. The depth of penetration at constant speed was found to be linearly dependent in the diameter of the indenter, varying over the range up to 2 mm. Thus, a simple normalization of displacement with diameter makes the stress–penetration relation independent of indenter size.

3. The slope of log–log plot of stress–penetration curve was found to be the same as that of compression tests.

4. Using a constant multiplying factor for stress and also for penetration of the impression test curves, a good agreement was found between stress–strain curves of compression test and the equivalent stress–penetration curves of impression test.

5. This is a relatively easy method to obtain the stress–strain relation and can detect the strain rate effect.

Acknowledgement

Helpful discussions with Professor J. C. M. Li of University of Rochester are gratefully acknowledged. Appreciation is extended to Dr S. C. Sanday and Dr A. Pattnaik during the conduct of the experiment.

References

1. H. O'NEILL, "Hardness Measurement of Metals and Alloys" (Chapman and Hall, London, 1967), p. 10.

2. S. N. G. CHU and J. C. M. LI, *Mater. Sci. Eng.* **45** (1980) 167.
3. I. GUPTA and J. C. M. LI, *ibid.* **6** (1970) 20.
4. H. O'NEILL and H. GREENWOOD, *J. Inst. Met.* **48** (1932) 47.
5. E. C. YU and J. C. M. LI, *Phil. Mag.* **36** (1977) 811.
6. H. HENCKY and F. ANGEW, *Math. Mech.* **31** (1923) 241.
7. A. J. ISHLINSKY, *J. Appl. Math. Mech.* (USSR) **8** (1944) 233.
8. R. T. SHIELD, *Proc. R. Soc.* **233** (1956) 267.
9. G. EASON, R. T. SHIELD and F. ANGEW, *Math. M. Phys.* **11** (1960) 33.
10. J. W. HARDING and L. N. SNEDDON, *Proc. Cambridge Phil. Soc.* **41** (1945) 16.
11. D. TABOR, *Proc. R. Soc.* **A192** (1948) 247.
12. A. G. ATKINS and D. TABOR, *J. Mech. Phys. Solids* **13** (1965) 149.
13. N. A. STIDWELL and D. TABOR, *Proc. Phys. Soc.* **78** (1961) 169.
14. L. SAMUELS and T. MULHERN, *J. Mech. Phys. Solids* **5** (1957) 125.
15. S. N. G. CHU and J. C. M. LI, *J. Mater. Sci.* **12** (1977) 2200.
16. H. Y. YU and J. C. M. LI, *ibid.* **12** (1977) 2214.

Received 28 November 1983
and accepted 12 April 1984